



Contents lists available at ScienceDirect

Quaternary Science Reviews

journal homepage: www.elsevier.com/locate/quascirev

A bi-polar signal recorded in the western tropical Pacific: Northern and Southern Hemisphere climate records from the Pacific warm pool during the last Ice Age

Reetta Saikku^{a,*}, Lowell Stott^a, Robert Thunell^b

^a Department of Earth Sciences, University of Southern California, Los Angeles, CA 90089, USA

^b Department of Geological Sciences, University of South Carolina, Columbia, SC 29208, USA

ARTICLE INFO

Article history:

Received 12 December 2008

Received in revised form

24 April 2009

Accepted 4 May 2009

ABSTRACT

Western tropical Pacific sea surface temperatures and Pacific Deep Water temperatures during Marine Isotope Stage 3 have been reconstructed from the $\delta^{18}\text{O}$ and Mg/Ca of planktonic and benthic foraminifera from *Marion Dufresne* core MD98-2181. This 36 m marine core was collected at 6.3°N from a water depth of 2114 m. With sediment accumulation rates of up to 80 cm/ky, it provides a decadal resolved history of ocean variability during the Last Glacial period. Surface temperatures and salinities at this site varied in close association with millennial-scale atmospheric temperature swings at high northern latitudes as reflected in the GISP2 ice core. At times of colder atmospheric temperatures over Greenland, the western Pacific was more saline and summer season SSTs were ~ 2 °C colder. These millennial-scale changes within the tropics are attributed to a southward displacement of the summer season ITCZ in response to steeper meridional temperature gradients within the Pacific. The benthic $\delta^{18}\text{O}$ record from MD98-2181 documents upper Pacific Deep Water temperature and salinity variability. Benthic $\delta^{18}\text{O}$ variations of 0.3–0.5‰ during MIS 3 indicate deep waters within the Pacific were varying by ~ 1 –1.5 °C, with the possibility that some of the variability was due to changing salinity and minor glacial–eustatic changes. The observed deep-water variability correlates to changes in Antarctic surface temperatures and thus reflects changes in Southern Ocean temperatures at the site of Pacific Deep Water formation. The combined planktonic and benthic records from MD98-2181 thus provide a northern and southern hemispheric climate record of anti-phased variability during MIS 3 as has been inferred previously from ice core records. Furthermore, the deep sea temperature excursions appear to have led millennial variations in atmospheric CO_2 as recorded in the EDML ice core by ~ 1 kyr.

© 2009 Elsevier Ltd. All rights reserved.

1. Introduction

Between 60 and 30 kyBP Earth's climate underwent recurrent, millennial-scale fluctuations. Synchronization of $\delta^{18}\text{O}$ records from Greenland and Antarctic ice cores using atmospheric methane stratigraphy indicates atmospheric warming over Antarctica during cooling stages in Greenland (Blunier and Brook, 2001). This difference in timing of millennial-scale climate variations occurred repeatedly during the Last Glacial despite an overall cooling trend and build-up of continental ice (Barbante et al., 2006; Raisbeck et al., 2007). Since their discovery from ice core records in Greenland and Antarctica, these millennial-scale hemispheric climate oscillations have been documented in other climate proxy records. This includes stalagmite, lake and marine records from around the globe (Behl and Kennett, 1996; Schulz et al., 1998;

Sirocko et al., 1999; Wang et al., 2001; Altabet et al., 2002; Burns et al., 2003; Genty et al., 2003; Martrat et al., 2004; Cruz et al., 2005). Sea surface temperature (SST) and salinity (SSS) in the tropics were also changing in concert with the high latitude temperature variations (Stott et al., 2002; Pahnke and Zahn, 2005) by up to 2 °C in SST and 2 in salinity. In the Cariaco Basin, an anoxic basin located off the northern coast of Venezuela, correlations between Greenland $\delta^{18}\text{O}$ and sediment color (which is largely a function of organic matter content) imply that surface productivity along the Venezuelan coast varied both in timing and abruptness with Greenland temperature variations in response to variations in trade wind strength and upwelling (Haug et al., 2001). Over Asia the summer monsoon rainfall was higher during interstadials and lower during the colder stadials (Wang et al., 2001). Ocean circulation changes were also recorded in high resolution marine sediment cores from the Iberian margin which contain a record of the different water masses, which came from the northern North Atlantic and Antarctic regions. Millennial deep-

* Corresponding author: Tel.: +1 213 740 6733; fax: +1 213 740 8801.
E-mail address: saikku@usc.edu (R. Saikku).

water temperature changes, potentially up to 1–1.5 °C, and $\delta^{18}\text{O}_{\text{dw}}$ variations recorded from the Iberian Margin describe an alternation between two relatively invariant colder and warmer deep-water end-members. This suggests the changing of local dominance from northern-sourced NADW to southern-sourced AABW (Shackleton et al., 2000; Martrat et al., 2007). Stott et al. (2002) presented a Late Pleistocene history of seawater surface variability in temperature and salinity from the western tropical Pacific warm pool that appeared to vary in accord with these millennial-scale stadial–interstadial cycles (Dansgaard/Oeschger cycles) over Greenland. Positive excursions in $\delta^{18}\text{O}_{\text{sw}}$ showed that tropical salinities in the Pacific warm pool increased during high latitude stadials whereas during interstadials surface salinities decreased (Stott et al., 2002). In a recent study of deep-water temperature change during the last deglaciation Stott et al. (2007) found that deep waters within the Pacific began to warm ~1000 years earlier than tropical surface waters. This lead–lag relationship was interpreted to reflect an earlier warming in the Southern Ocean at the location where Pacific Deep Water acquires its temperature. This deep-water lead was interpreted to reflect a Southern Ocean response to increased spring season insolation that influenced sea ice (Timmermann et al., 2009).

Despite a growing number of high resolution paleoclimate records of millennial climate variability within the Northern Hemisphere, there still remain relatively few high resolution marine or terrestrial records from the Southern Hemisphere. Consequently, it is not clear if the entire Southern Hemisphere participated in the anti-phased climate swings that are reflected in ice core reconstructions. In particular, it is not known how deep-water temperatures within the Pacific were affected by these high latitude temperature variations on millennial to centennial time-scales. Examination of this scale of variation is important in terms of identifying feedbacks operating with different time constants within the climate system, such as the role of the thermohaline circulation. In the present study we expand on previous findings and attempt to evaluate the timing and extent of deep sea and tropical surface water temperature changes during the Last Glacial period and determine whether the anti-phased relationship between Southern Hemisphere (Deep Pacific) and Northern Hemisphere (tropical surface water) is evident.

2. Regional setting and oceanography

2.1. Surface water

Marine core MD98-2181 was collected aboard the *Marion Dufrenoy* in 1998 as part of the IMAGES coring program and is composed of fine-grained, brown to gray hemi-pelagic sediments that are uniform in appearance. At 6.3°N, 125.83°E, MD98-2181 is located in the Morotai Basin in the western tropical Pacific at a water depth of 2114 m (Fig. 1.). At this depth, the preservation of foraminifera is very good. The western Pacific warm pool (WPWP) is an important center of atmospheric convection with surface temperatures within the warm pool today in excess of 28 °C. In contrast, sea surface temperatures in the eastern equatorial Pacific are relatively cool (~20 °C), resulting in a large zonal sea surface temperature (SST) gradient across the equatorial Pacific. The western tropical Pacific and the East Asian monsoon region are linked by the seasonal migration of the Intertropical Convergence Zone (ITCZ). During the boreal summer (July to September) the northward movement of the ITCZ brings southerly/southeasterly winds across the Indonesian maritime continent and East Asia. It is during this season that the western tropical Pacific receives the greatest rainfall, as much as 300 and 400 mm/month during summer (Stott et al., 2002). The boreal winter season is

characterized by a reversal in the winds across the maritime continents of the western Pacific (Gordon, 2005). These seasonal wind patterns are associated with marked changes in surface water properties including temperature and salinity. In the region of Mindanao, during the northern summer SSTs in the western Pacific warm pool average 29–30 °C and in winter, SSTs cool to 26–27 °C (Gordon, 2005). The sea surface salinities (SSS) annually range between 33.8 and 34.2 (Gordon, 2005). Because of its great topographic relief and active tectonics, this region contributes large amounts of water, solutes, and sediment to the coastal ocean (Nittroauer et al., 1995).

2.2. Deep-water masses

The primary water masses in the Pacific Ocean Basin are the Antarctic Intermediate Water (AAIW), Antarctic Bottom Water (AABW) and the Upper and Lower Circumpolar Deep Water (UCDW and LCDW) or Pacific Deep Water (PDW) (Fig. 1b). North Atlantic Deep Water (NADW) mixes with recirculated deep water from the Indian and Pacific Oceans, forming a relatively warm deep-water mass, the Circumpolar Deep Water (CDW), overlying the colder AABW. Today the main export pathway of CDW and modified AABW from the Antarctic Circumpolar Current (ACC) to the Pacific is the Deep Western Boundary Current (DWBC) (van de Flierdt et al., 2004). The DWBC passes along the Tonga–Kermadec trench, up the western Pacific island arc, turning clockwise north of the equator and filling the entire deep North Pacific. Eventually, this modified water mass returns southward at mid-depths as UCDW identified by an oxygen minimum at 2–3 km depth and LCDW which is marked by a faint salinity maximum (Fig. 1b). The Antarctic deep-water masses flowing northward have initial radiocarbon ages of ~700 years for intermediate waters and ~1400 years for bottom waters (Ostlund and Stuiver, 1980; Sikes et al., 2000). The subsurface return flow of UCDW and LCDW from the north in the Pacific has ages of ~1500–2000 years at mid-depths (Ostlund and Stuiver, 1980; Sikes et al., 2000). Located in the western tropical Pacific site MD98-2181 is bathed in UCDW or Pacific Deep Water. The neutral density surface $\gamma^n = 27.9 \text{ kg/m}^3$ (relative to the 0 m reference level) outcrops in the Southern Ocean near the Polar Front and attains a depth of about 2000 m near the MD98-2181 core location. The UCDW flows between $\gamma^n = 27.4\text{--}28.0$ (Rintoul et al., 2001). Therefore the oxygen isotope composition of benthic foraminifera at MD98-2181 varies in response to changes in water mass properties (temperature and $\delta^{18}\text{O}_{\text{sw}}$) of the southern source waters. In combination with a Northern Hemisphere climate signature from the planktonic foraminiferal $\delta^{18}\text{O}$ and Mg/Ca, the data from MD98-2181 provides a climate record for both hemispheres at a single location.

3. Materials and methods

3.1. Sample preparation and analysis

All of the MD98-2181 planktonic and benthic data presented here is new; the core was completely resampled with u-channels, which provide continuous, centimeter resolution. The sediment samples were disaggregated in sodium hexameta phosphate solution. Once disaggregated, the sediments were wet-sieved through a 63 μm mesh to remove the clay fraction. The >63 μm fraction was then dry-sieved at 180 μm size fraction. The planktonic foraminifer *Globigerinoides ruber* (white) and the benthic foraminifer *Uvigerina hispida* were picked from the >180 μm sieved samples for isotopic and Mg/Ca determinations. *Globigerinoides ruber* (white) is a surface-dwelling planktonic foraminifera that produces carbonate shells throughout the year in the western tropical Pacific and appears to

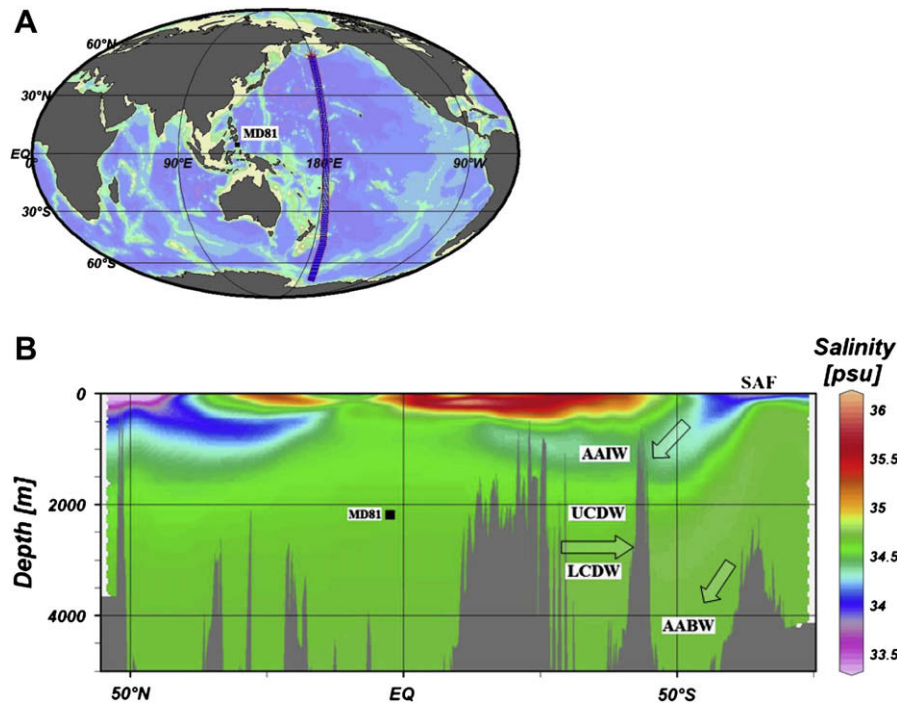


Fig. 1. (A) Map showing location of MD98-2181 and a N-S salinity transect. (B) Salinity of the Pacific Ocean along N-S transect and depth and location of MD98-2181. Water masses Antarctic Intermediate Water (AAIW), Upper Circumpolar Deep Water (UCDW), Lower Circumpolar Deep Water (LCDW) and Antarctic Bottom Water (AABW) are shown at their appropriate depths. SAF, Sub-Antarctic Front.

precipitate calcite in isotopic equilibrium with surface waters (Kawahata et al., 2002; Kawahata, 2005). The benthic foraminifera *Uvigerina hispida* has a shallow infaunal habitat (Boersma, 1984). The foraminifera were cleaned according to a protocol that is designed to remove clays and other impurities. The foraminiferal shells were cracked between two glass plates under the microscope to open the tests. The tests were then rinsed with DIW, methanol, hot alkaline oxidative cleaning using buffered hydrogen peroxide and a leach with 0.001 M nitric acid. During each of the rinses the vials were sonified to dislodge debris from the shells. The cleaned *G. ruber* samples were split for isotope and Mg/Ca measurements. This ensured that isotopic and minor element measurements were made on the same samples of cleaned calcite, and eliminated potential discrepancies due to the effects of different cleaning methods on measured Mg/Ca and $\delta^{18}\text{O}$. For Mg/Ca analyses, the samples were dissolved in 500 μL of 1 M nitric acid and analyzed on a Jobin Yvon ICP AES. Each sample measurement was bracketed with a standard that was made from solid Mg and reagent grade CaCO_3 in an elemental ratio of 5.62 mmol/mol and the sample value was adjusted by the standard deviation of the two bracketing standards to correct for within and between run instrument drift. The average sample standard deviation was 0.05 mmol/mol. The main uncertainty is introduced via the conversion of planktonic Mg/Ca to an SST estimate using the Mg/Ca temperature calibration of Anand et al. (2003) for *G. ruber* (white), with an estimated accuracy of ± 1.2 °C. Diagenetic alteration of CaCO_3 is a potential concern because it can modify the original isotopic and Mg/Ca signature. During the picking of foraminifera from core MD98-2181 the foraminifera did not fragment on contact. Also, the cleaning procedure caused only minimal fragmentation. Careful visual examination using microscopy indicated the site contains well-preserved biogenic carbonate. At a depth of 2114 m, MD98-2181 is above the lysocline and has a high sediment accumulation rate. Small amounts of terrigenous contamination that are not removed by cleaning or the presence of

authigenic phases (such as Mn-Fe oxides, pyrite, and secondary minerals such as ferric oxyhydroxides) can affect the Mg/Ca paleothermometry. The efficacy of our cleaning procedure was evaluated continuously by measuring Fe and Mn in all *G. ruber* samples analyzed. Fe (ppb) and Mn (ppb) values for 100 randomly chosen Mg/Ca data points between core depths of 1836 and 3102 cm were plotted to check for any correlation between the Fe and Mn and Mg/Ca values. Mn and Fe exhibited no positive correlation with Mg/Ca measured in *G. ruber* suggesting that contamination is not a significant influence on Mg/Ca variability. For stable isotopic measurements the samples were analyzed on a VG Prism II stable isotope ratio mass spectrometer equipped with a common acid bath acidification system. Approximately 30 foraminiferal samples are run sequentially on the mass spectrometer along with approximately 10 Ultissima marble standards that are used to monitor analytical precision in the University of Southern California isotope laboratory. In the present study the precision of the Ultissima standard $\delta^{18}\text{O}$ was 0.06‰ with a 1σ of 0.068‰ over 17 runs. To calculate $\delta^{18}\text{O}_{\text{sw}}$ the equation of Bemis et al. (1998) was used. The data was further corrected for the long-term global $\delta^{18}\text{O}_{\text{sw}}$ variations due to global ice volume (using Siddall et al., 2003 data), in order to extract the regional $\delta^{18}\text{O}_{\text{sw}}$ signal ($\Delta\delta^{18}\text{O}_{\text{sw}}$).

3.2. Age models

The age model for the MD98-2181 core is based on AMS ^{14}C age dates to a core depth of 1711 cm (Stott et al., 2007), approximately 28 kyrBP. This ^{14}C -based age model was derived from the depth-calibrated ^{14}C ages using the CALIB 5.0.2 with the Marine04 calibration relationship as outlined in Stott et al. (2007). The reservoir age correction for tropical surface waters was 480 years for samples younger than 13,000 years BP and 630 years for older samples. The ^{14}C age for the 12 cm interval is 580 years and indicates the top of this core has a ~ 0 kyrBP age. An age/depth plot of these calibrated

ages indicates a continuous and approximately linear sediment accumulation rate through the Late Holocene (~170 cm/kyr). The sediment accumulation rate was lower but also approximately constant during the Last Glacial between 10 and 25 kyrBP (~50 cm/kyr). Extrapolating the Late Glacial ^{14}C age/depth relationship through the glacial portion of the core reveals systematic variations in planktonic foraminiferal $\delta^{18}\text{O}_c$ that closely match the timing of temperature changes over Greenland (Stott et al., 2002). In the present study we made small adjustments to this age/depth curve through the stage 3 section by aligning the minima and maxima of the *G. ruber* $\delta^{18}\text{O}_c$ to the temperature maxima and minima respectively in the GISP2 $\delta^{18}\text{O}$ record (Blunier and Brook, 2001) (Fig. 2). These stratigraphic tie-points are the maximum and minimum ice core temperatures of D/O events 4–15 (excluding D/O events 9, 13 and 14 where only the maxima have been used) as well

as the Laschamp excursion at ~41 ka (Fig. 2). In this way the planktonic $\delta^{18}\text{O}$ record of MD98-2181 is tied to the GISP2 age model. This dating strategy has been independently confirmed by the comparison of geomagnetic field relative paleointensity between the MD98-2181 and an independently dated sediment core from the North Atlantic with an error of ± 300 years at each D/O event (Stott et al., 2002; S. Lund, personal communication, 2008).

3.3. Planktonic–benthic $\delta^{18}\text{O}$ age offset

A reservoir age correction for tropical surface waters of 630 years was applied to samples older than 13,000 years BP (Stott et al., 2007). A reservoir age for glacial sub-polar surface waters within the Southern Ocean, the source region for Pacific Deep Water, is estimated to be 560 ± 40 years (Sikes et al., 2000). The tropical surface water to

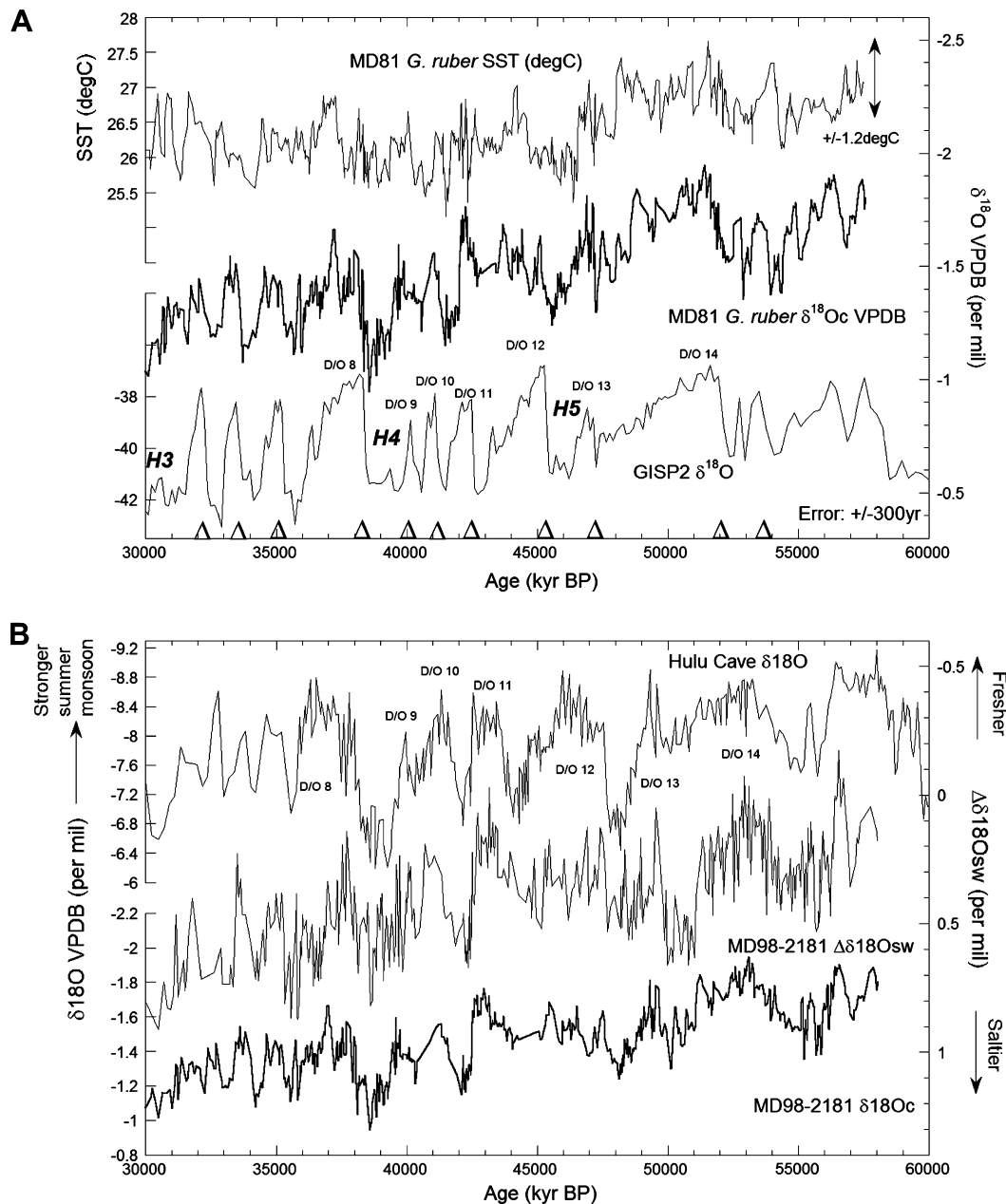


Fig. 2. (A) GISP2 $\delta^{18}\text{O}$ (Blunier and Brook, 2001; Ahn and Brook, 2007), *G. ruber* SST ($^{\circ}\text{C}$) and $\delta^{18}\text{O}_c$ plotted with respect to the GISP2 age scale. Error scale of ± 1.2 $^{\circ}\text{C}$ is depicted by the arrow. Triangles depict location of tie-points used to construct age model with an error of ± 300 years. (B) Hulu Cave $\delta^{18}\text{O}_{VPDB}$ (Wang et al., 2001), MD98-2181 $\Delta\delta^{18}\text{O}_{sw}$ and $\delta^{18}\text{O}_c$ plotted with respect to the Hulu stalagmite age scale.

upper Pacific Deep Water ^{14}C age difference today is approximately 1400 years and was ~ 1500 years (1482 ± 367 years) during the Late Glacial and termination, based on AMS dates on coexisting planktonic–benthic foraminifera from MD98-2181 (Broecker et al., 2004; Stott et al., 2007). The work by Butzin et al. (2005) with ocean model sensitivity experiments also showed that the surface-to-deep-water ^{14}C age difference in the western tropical Pacific was not significantly changed (1000 ± 100 years) by glacial/interglacial climate changes such as changing winds, brine release in the Southern Ocean and North Atlantic melt water pulses. Stott et al. (2007) estimated the propagation time of deep water from its source region near the Southern Ocean to MD98-2181 in the western tropical Pacific to have remained relatively constant throughout the previous glacial termination based on the constant benthic–planktonic ^{14}C differences. The present-day propagation time of deep waters from their source region to the tropical Pacific can be roughly estimated from the prebomb- ^{14}C distribution in the Pacific using the GLODAP carbon isotope climatology (Key et al., 2004). Eddy mixing, convection and Ekman transport mix deeper and older ocean waters with surface waters south of 50°N , which enhances the reservoir age of the Pacific deep waters. Between the Antarctic and the northern equatorial Pacific the ^{14}C age of Pacific deep water increases from ~ 800 – 1000 years to about ~ 1900 years at 10°N , suggesting a propagation time of between 900 and 1100 years (Stott et al., 2007). It should be noted however, that ^{14}C is not a pure advective tracer because it is subject to ocean interior mixing. The estimated time required for deep waters to travel between the Southern Ocean and the north equatorial Pacific based on the ^{14}C gradients depicted in modern observational data set is also consistent with ocean model estimates of a transit time of ~ 800 – 1000 years (Broecker et al., 2004). Combining the modern observational data, paleo-proxy data and model estimates for modern circulation in the Pacific, the transit time from the Southern Ocean to MD98-2181 is therefore estimated to be ~ 1000 years (± 300 years) during the Glacial, the same as it is today. This study therefore applies a 1000 year lead in benthic (deep water) $\delta^{18}\text{O}_c$ record to the planktonic $\delta^{18}\text{O}_c$ record. The estimated transit time of 1000 years for the Last Glacial period could therefore be considered a minimum estimate if the increased ^{14}C during the Glacial reflects a longer transit time for deep water circulating between the Southern Ocean and the northern tropical Pacific (Stott et al., 2007).

4. Results

4.1. MD98-2181 planktonic record

The planktonic foraminiferal Mg/Ca SST and $\delta^{18}\text{O}$ records from MD98-2181 are compared to the Hulu Cave stalagmite (Wang et al., 2001) and the GISP2 Greenland ice core (Blunier and Brook, 2001; Ahn and Brook, 2007) records in Fig. 2. Planktonic *G. ruber* $\delta^{18}\text{O}_c$ and SSTs in the western tropical Pacific varied by up to 0.8‰ (-1 to -1.8‰) and 2°C , respectively, throughout the D/O events of stage 3. These tropical Pacific variations coincided closely with the shifting monsoon rainfall over Asia as reflected in the Hulu Cave isotope reconstruction and with the atmospheric temperature changes over Greenland (Fig. 2). Estimates of surface water $\Delta\delta^{18}\text{O}_{\text{sw}}$ derived from the *G. ruber* $\delta^{18}\text{O}_c$ and SST data also follow the millennial-scale oscillations. According to the modern $\delta^{18}\text{O}_{\text{sw}}$ –salinity relationship in the tropical Pacific a decrease in $\Delta\delta^{18}\text{O}_{\text{sw}}$ of $\sim 0.5\text{‰}$ signifies a decrease in sea surface salinity of ~ 1 – 1.5 (Fairbanks et al., 1997; Morimoto et al., 2002).

Our western tropical Pacific SST record documents a long-term cooling between 60 and 38 ka (Fig. 2). This sustained downward trend in SSTs appears to have leveled off by ~ 38 ka when SSTs reached their lowest values during MIS3. The D/O events in the Greenland ice core record, and the approximate timing of the

Heinrich (H) events H3 at ~ 31 ka, H4 at ~ 38 ka and H5 at ~ 45 ka (Hemming, 2004) are indicated in the figure.

The large oscillations evident in both *G. ruber* $\delta^{18}\text{O}_c$ and $\Delta\delta^{18}\text{O}_{\text{sw}}$ (corrected for sea level variations, proxy for regional SSS) at MD98-2181 (Fig. 2) and the Asian monsoon speleothem records implies a close temporal coupling between the tropical Pacific ocean/atmospheric changes and the high northern latitude temperature variability. However, there are also notable differences between the low and high latitudes in the rate of temperature change at the beginning of millennial warm events during MIS 3. This is particularly evident at the beginning of D/O 14 and D/O 12 in the Greenland ice core record. In the North Atlantic interstadial warming was abrupt whereas in Asia and the tropical Pacific higher precipitation and SST warming were more gradual and may have begun to change earlier (Fig. 2). This is also the case for the D/O 12 (Fig. 2). These differences in the rate of change at the beginning of millennial warm events are not an artifact of the way the MD98-2181 age model was constructed.

4.2. MD98-2181 benthic record

The MD98-2181 benthic $\delta^{18}\text{O}$ record documents millennial-scale variations of 0.3 – 0.5‰ , with rapid shifts from more depleted to more isotopically enriched values throughout MIS3 (Fig. 3). If these $\delta^{18}\text{O}$ shifts were due entirely to temperature change in the deep Pacific they would translate to ~ 1 – 1.5°C ($\sim 0.3\text{‰}$ per $^\circ\text{C}$). The abruptness of some of these events is especially striking. For example, between ~ 32 and 42 ka there were changes of 0.3 – 0.5‰ over approximately a century. At a depth of 2114 m, the benthic foraminifera are recording changes in Southern Ocean-sourced waters. The timing of these events in the MD98-2181 record must therefore take into account the transit time between the Southern Ocean and the location of MD98-2181. A 1 ka age offset relative to the planktonic ages is applied to the MD98-2181 benthic data to account for the transit time. The time adjusted MD98-2181 benthic $\delta^{18}\text{O}$ record is then compared to the Antarctic Dome Fuji (Kawamura et al., 2007) and Byrd (Blunier and Brook, 2001) ice core $\delta^{18}\text{O}_{\text{VSMOW}}$ in order to assess how the timing of events in the deep Pacific compares with Antarctic air temperature changes reflected in the ice core records (Fig. 3). The age adjusted MD98-2181 benthic $\delta^{18}\text{O}$ record is quite similar to the pattern of Antarctic $\delta^{18}\text{O}$ variability during the Last Glacial. The gradual warming evident in the millennial temperature swings over Antarctica that are evident in the Dome Fuji (Kawamura et al., 2007) and Byrd (Blunier and Brook, 2001) ice cores between ~ 45 and 60 ka (such as events A2 and A3) are also seen in the MD98-2181 benthic $\delta^{18}\text{O}$ record. This is in marked contrast to the more rapid oscillations in surface water variables in the MD98-2181 planktonic foraminiferal records ($\delta^{18}\text{O}$ and Mg/Ca SST) that are typical of Northern Hemisphere millennial-scale changes during MIS 3.

The benthic $\delta^{18}\text{O}$ values increased gradually between 60 and 40 ka and then decreased between 40 and 30 ka indicating moderate warming (as well as a potential salinity and ice-volume component), similar to what is seen in the MD98-2181 planktonic isotope record. The degree of correspondence between the MD98-2181 record and the Antarctic ice core record is not as clear between 30 and 40 ka.

5. Discussion

5.1. Planktonic records – Northern Hemisphere and monsoon variability

Globigerinoides ruber $\delta^{18}\text{O}$ and Mg/Ca SST changes of up to 0.8‰ (-1 to -1.8‰) and 2°C , respectively, occurred in the western tropical Pacific during MIS3. These temperature changes were

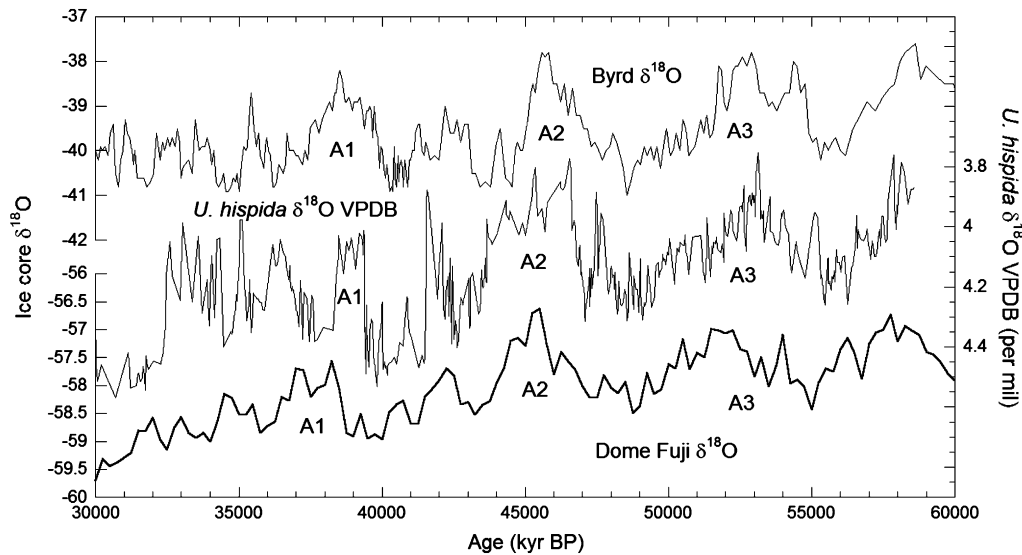


Fig. 3. *U. hispidia* $\delta^{18}\text{O}_{\text{VPDB}}$ plotted against Antarctic ice core $\delta^{18}\text{O}$ from Dome Fuji (Kawamura et al., 2007) and Byrd (Blunier and Brook, 2001) with respect to the GISP2 age scale.

accompanied by shifting surface water $\Delta\delta^{18}\text{O}_{\text{sw}}$. The close correspondence between the MD98-2181 $\delta^{18}\text{O}_{\text{c}}$, SST and $\Delta\delta^{18}\text{O}_{\text{sw}}$ variations, and Hulu Cave stalagmite records with the millennial oscillations seen in the Greenland ice core history implies a strong northern hemisphere influence on the hydroclimate of the tropical Pacific. The Hulu Cave speleothem record of Wang et al. (2001) was interpreted to reflect variations in monsoon rainfall over China during the Last Glacial; lower $\delta^{18}\text{O}$ values in the speleothem calcite signifying more intense summer monsoon (June–September) precipitation. Greenland temperature increases correlate positively with greater summer (June–September) precipitation in eastern China. On the basis of their own independent time scale, it appears that increased summer monsoon precipitation was synchronous with atmospheric warming over the northern high latitudes (Wang et al., 2001). The stronger summer monsoon and increased summer precipitation (more depleted $\delta^{18}\text{O}_{\text{VPDB}}$ values) at Hulu Cave coincided with fresher (lower $\delta^{18}\text{O}_{\text{sw}}$) and warmer conditions in the western Pacific warm pool. Other cores from the western Pacific also reveal large sea surface temperature and salinity changes during the glacial that have been interpreted to reflect a hydrologic response to the changes in the monsoon circulation (Pelejero et al., 1999; Lea et al., 2000; Dannenmann et al., 2003).

5.1.1. ITCZ movement and possible implications for ENSO during MIS 3

The mean position of the ITCZ is controlled by the seasonal pole-to-equator temperature gradient and the regional ocean–land distribution across the equator. The seasonal motion of the ITCZ is accompanied by large changes in rainfall in the tropics. In the tropical Atlantic for example, negative rainfall anomalies occur in northeastern Brazil in response to negative SST anomalies in the southern tropical Atlantic and positive anomalies in the northern tropical Atlantic (Wang et al., 2004); a pattern that is associated with a northward displacement of the ITCZ during boreal summer. Temperature anomalies in the opposite direction strengthen the northeast trade winds and cause a southward shift in the ITCZ during boreal winter. This is accompanied by enhanced rainfall over northeastern Brazil (Wang et al., 2004). In their study of the rainfall patterns during MIS 3, Wang et al. (2004) found that wet periods in NE Brazil were synchronous with periods of weaker East Asian summer monsoons, cold stadials in Greenland and Heinrich events in the North Atlantic. Changes to the annual ITCZ cycle may

therefore serve as an appropriate basis for explaining the SST and SSS changes observed in the MD98-2181 record. Cooler surface waters in the western Pacific during stadials would be consistent with a southerly bias in the annual migration of the ITCZ. New terrestrial records from Lynch's Crater, Australia (Muller et al., 2008) appear to support this interpretation of the MD98-2181 results. Similarly, Stott et al. (2004) and Newton et al. (2006) previously attributed the long-term evolution of SSTs and SSSs within the Indo-Pacific warm pool during the Holocene to the latitudinal shift in the seasonal reach of the ITCZ.

A shift in the mean position of the ITCZ throughout the year can also influence surface salinities in the western tropical Pacific by modulating the seasonal hydrologic cycle and also modulating the transport of water vapor between the Atlantic and Pacific Basins (Stott et al., 2004; Oppo et al., 2007). Today there is net export of water vapor from the Atlantic Basin to the Pacific Basin across Central America during boreal summer when the ITCZ is at a northerly latitude and this contributes to the lower salinities within the Pacific Basin. During the Northern Hemisphere stadials, increased salinities are observed in the EEP (Leduc et al., 2007), coinciding with higher salinities in WEP (this study). If these records are characteristic of how the Pacific Basin salinities varied on these time scales this would be consistent with a southern bias in the latitude of the summer ITCZ and reduced vapor transport from the Atlantic. Model simulations agree with this interpretation of the paleo-observations, suggesting that the mean salinity of the Pacific was indeed higher due to a reduction in water vapor transported from the Atlantic Ocean (Xie et al., 2008). In their model results, Xie et al. (2008) observed that cooler North Atlantic temperatures are associated with higher sea level pressures that produce northeasterly wind anomalies that advect cooler and also drier air from the North Atlantic towards the Pacific. These anomalous northeasterly winds across Central America appear to be a robust feature of various water-hosing model experiments (Xie et al., 2008).

It is not yet clear how the temperature changes in the Northern and Southern Hemispheres during MIS 3 were manifest in the annual and interannual SST gradients and wind fields over the equatorial Pacific because a comprehensive network of highly resolved SST reconstructions does not yet exist for this time interval. The most highly resolved temporal reconstructions of tropical Pacific temperatures through the Last Glacial cycle are

currently limited to sites located north of the equator. And as summarized above, the proxy reconstructions at these sites do not resolve the annual or seasonal variability adequately. They represent a time averaged record of variability that is a complex function of how the proxies are produced (seasonal production cycles) in the surface ocean throughout the year and how these biological organisms respond to ecologic variability, including temperature change. In some instances the biological and ecological factors that control the proxy record are well understood in the modern ocean and this understanding can inform paleo-reconstructions that are derived from down core reconstructions. For example, Koutavas et al. (2002) used $\delta^{18}\text{O}$ and Mg/Ca measurements of surface-dwelling planktonic foraminifera isolated from sediment samples taken from a core collected in the eastern equatorial Pacific to deduce how sea surface temperatures varied during the Last Glacial maximum and from this inferred how the interannual variability during the Last Glacial maximum compared with more recent intervals in the Holocene. The foraminiferal values are taken to be representative of conditions at all times during the various phases of natural seasonal to interannual variability, including the El Niño and La Niña phases. In their study Koutavas et al. found that at the Last Glacial, maximum sea surface temperatures within the eastern equatorial Pacific cold tongue cooled by only $\sim 1.5^\circ\text{C}$, whereas outside the cold tongue equatorial SSTs cooled by nearly 3°C . From these results it was inferred that the tropical Pacific was characterized by a sustained El Niño-like state during the LGM. In another study of early Mid Holocene sections of cores from the tropical eastern Pacific analysis of individual planktonic specimens revealed a drastic $\sim 50\%$ reduction in $\delta^{18}\text{O}$ variance among single specimens isolated from the core samples, which was taken to indicate a severe reduction in ENSO variability (Koutavas et al., 2006). In the Mid Holocene the reduced variance was attributed to the northerly bias in the ITCZ annual cycle with more persistent southeasterly winds that sustained strong upwelling in the eastern equatorial Pacific. In case of the LGM and Mid Holocene a southerly and northerly bias in the ITCZ respectively, were associated with a change in the annual cycle and reduced ENSO variance. A similar approach may be possible for the MIS 3 intervals from cores collected in the northeastern equatorial Pacific where there is sufficient temporal resolution to identify stadials and interstadials (Leduc, personal communication). However, whereas Koutavas found significantly reduced ENSO-style variance in the Early–Mid Holocene in the eastern equatorial Pacific core near the Galapagos Islands, the core studied by Leduc et al. (personal communication) does not show a comparably large reduction in variance in early Holocene intervals. Hence, there are clearly important ecological and biological influences that regulate the production and also environmental signature that is embedded in individual foraminifera that must be resolved in order to derive a composite reconstruction of the annual to interannual variability in the tropical Pacific at all time scales.

In the present study we take clues from modern ocean/atmospheric behavior that document stronger equatorial upwelling in the eastern equatorial Pacific in boreal summer when the ITCZ lies over the northern tropics and the winds across the southeast Pacific are strong. Cooler SSTs in the western Pacific and a southerly bias in the ITCZ over the eastern Pacific (Leduc et al., 2009) during stadials could imply that SST gradients between the eastern and western Pacific were reduced. In this sense the MIS 3 stadials may have been characterized by a more El Niño-like state, similar to that observed for the LGM (Koutavas et al., 2002). On the other hand, the magnitude of the SST cooling in the western tropical Pacific during stadials was large, on the order of $1\text{--}1.5^\circ\text{C}$. If ocean/atmospheric feedbacks, including cloud feedbacks, strongly modulated the ocean's response, as climate models suggest, then there may have

been even greater cooling in the eastern equatorial upwelling region that enhanced the trade winds that reinforce the SST gradient and hence produced a larger east–west SST gradient across the Pacific. In this case, the tropical Pacific may have been more sensitive to ENSO variability. While such inferences about ENSO will require testing and verification, the asymmetric temperature changes between the Northern and Southern Hemispheres during MIS 3 D/O events may have influenced the amplitude of the annual cycle in the eastern Pacific, which is influenced by ocean–atmospheric feedbacks (Meehl and Washington, 1996; Timmermann et al., 2004) that are likely to have changed during the stadials and interstadials. There is a strong basis for considering how an increase or a decrease in amplitude of the annual cycle in the tropical Pacific would have influenced the frequency of ENSO events (Jin et al., 1994; Tziperman et al., 1994; Timmermann et al., 2004). In a coupled ocean/atmosphere model that is able to simulate ENSO, Clement et al. (2000) found that reduced ENSO variability would arise from an anomalous warming in the eastern equatorial Pacific relative to the western Pacific due to the ocean/atmospheric feedbacks, which in turn produces a positive feedback in the easterly winds that further cool the eastern equatorial Pacific in the fall season. In this sense, the isolation forcing reduces the annual cycle and suppresses the ENSO variability consistent with the mid Holocene reduction in ENSO-style variance observed in the $\delta^{18}\text{O}$ records from the eastern equatorial Pacific (Koutavas et al., 2006).

A globally coherent picture is now emerging of a southerly migration of the mean ITCZ position at times of colder conditions over Greenland and during Heinrich events in the North Atlantic. The southward bias in the ITCZ was also associated with a weaker East Asian summer Monsoon system, wetter conditions in eastern Brazil (Wang et al., 2004) and northern Australia (Muller et al., 2008), and a colder and more saline western tropical Pacific. Records of such ITCZ behavior as recorded by MD98–2181 show the importance and role of the equatorial region in global climate dynamics. Specifically, these results demonstrate unequivocally that changes in the East Asian monsoon and the hydrology of the tropics are linked on millennial timescales via atmospheric and oceanic circulation pathways to the northern high latitudes. These opposing patterns of precipitation between the northern and southern tropics have been hypothesized to be in response to high latitude forcing originating with dynamics of freshwater pulses and ice extent at the poles, or the result of tropical forcing. We believe however, it is premature to infer whether or not the interannual variability within the tropical Pacific was increased or decreased during the MIS 3 interval.

5.2. Benthic record – high southern latitudes

A 1 ka offset has been applied to the MD98–2181 benthic data from the MD98–2181 planktonic data to account for the deep-water travel time from the Southern Ocean to the western tropical Pacific. In applying this offset we are evaluating the timing of change at the source region where the deep waters obtain their temperature and salinity. With no other modification applied, the benthic data exhibits remarkable correlation with the Antarctic surface temperature history as recorded by the Byrd and Dome Fuji $\delta^{18}\text{O}$ (Fig. 3). The MD98–2181 benthic $\delta^{18}\text{O}$ record documents millennial-scale oscillations of $0.3\text{--}0.5\text{‰}$ signifying changes in temperature with a potential added salinity and/or sea level component. If the entire $\delta^{18}\text{O}$ shift was due to temperature changes it would translate to Pacific deepwater changes of between ~ 1 and 1.5°C ($\sim 0.3\text{‰}$ per $^\circ\text{C}$). Skinner and Elderfield (2007) found temperature excursions of up to 1.5°C in North Atlantic deep water as measured from benthic foraminifera occurring during Heinrich events in stage 3. Maximum sea level variation estimates during stage 3 range from $\sim 0.12\text{--}$

0.28‰ (Chappell, 2002; Siddall et al., 2003; Rohling et al., 2004; Arz et al., 2007), therefore the larger millennial variations in benthic $\delta^{18}\text{O}_c$ at MD98–2181 are not accounted for by variations in global ice-volume fluctuations, and must reflect hydrographic changes in temperature and salinity. According to Skinner and Shackleton (2005) the large volume of the deep Pacific combined with the relatively small lateral gradient of temperature/ $\delta^{18}\text{O}_{\text{dw}}$ would mean that large changes in local deep-water characteristics are most likely driven by changes in temperature and/or $\delta^{18}\text{O}$ at the source region where deep Pacific water is formed in the Southern Ocean. Also recent work by McCave et al. (2008) on cores from the Deep Western Boundary Current in the southwest Pacific demonstrated that the structure of Lower Circumpolar Deep Water–Upper Circumpolar Deep Water/North Pacific Deep Water–Antarctic Intermediate Water has remained constant over the past 160 ka with no apparent changes in the depth of water mass boundaries between glacial and interglacial states. Therefore our MD98–2181 results suggest that the Pacific Deep Water/UCDW was rapidly responding to climate perturbations in the Antarctic on short timescales. These signals may have been carried into the North Pacific via the primary water masses that form in the Pacific Basin (AAIW and AABW) with contributions from the NADW via mixing with recirculated deep water from the Indian and Pacific Oceans.

5.3. Evidence for a bi-polar seesaw in the Pacific

The phasing between high resolution (~ 50 yr/sample) $\delta^{18}\text{O}_c$ benthic and Mg/Ca and $\Delta\delta^{18}\text{O}_{\text{sw}}$ (regional SSS) planktonic records from MD98–2181 is shown in Fig. 4. The planktonic and benthic records each exhibit similar long-term changes that reflect the progressive cooling and ice build-up in the Northern Hemisphere throughout the Glacial. However, what is most striking about the comparison is the anti-phased pattern of variability between the tropical surface water and the high southern latitude deep-water records. This anti-phased relationship is also evident between the surface water salinity signal ($\delta^{18}\text{O}_{\text{sw}}$) and the benthic deepwater $\delta^{18}\text{O}$. The anti-phasing occurs at a timescale of 1–2 ka, which is consistent with the climate signal propagating through the oceans. Shifts

towards colder and/or more saline (more ^{18}O enriched) surface waters correspond to warming and/or a freshening (more isotopically depleted) Southern Ocean, the source region of Pacific Deep Water.

The ice core temperatures in Greenland and Antarctica were anti-phased during the Last Glacial period (Labracherie et al., 1989; Jouzel et al., 1995; Sowers and Bender, 1995; Blunier et al., 1997; Blunier et al., 1998). These differences in timing of millennial-scale temperature variations between the two hemispheres were a persistent characteristic of the Last Glacial period and were maintained throughout the Glacial despite the changing background state of the climate system (Blunier and Brook, 2001). Climate model studies have suggested that as the North Atlantic Deep Water (NADW) formation switches on or intensifies, heat from the Southern Hemisphere oceans is advected into the Northern Hemisphere leading to reduced temperatures in the south as Northern Hemisphere temperatures warm. This north–south heat transfer has been termed the “bi-polar seesaw” (Stocker et al., 1992; Broecker, 1998; Stocker, 1998; Stocker and Johnsen, 2003).

The MD98–2181 benthic and planktonic data plotted against GISP2 and Byrd ice core $\delta^{18}\text{O}$ (Blunier and Brook, 2001) in Fig. 5 suggests a similar northern and southern hemispheric anti-phased relationship, consistent with observations that have been made in the Atlantic (Martrat et al., 2007). The MD98–2181 planktonic and benthic data display an anti-phased relationship that is associated with a bi-polar seesaw oceanographic behavior throughout MIS 3. This is also in agreement with previous results from the deep northeast Pacific Ocean, where the benthic foraminiferal $\delta^{18}\text{O}$ signal showed warming roughly in unison with the Southern Ocean temperatures differing from the northeast Pacific planktonic signal (Mix et al., 1999).

5.3.1. Millennial-scale atmospheric and oceanographic climate fluctuation

The coupling of Greenland and North Atlantic temperatures has been proposed to involve perturbations to the thermohaline circulation system, which may behave in an “oscillatory” manner alternating between a dominant northern- or southern-sourced deep-water production factory (Duplessy et al., 1988; Charles et al.,

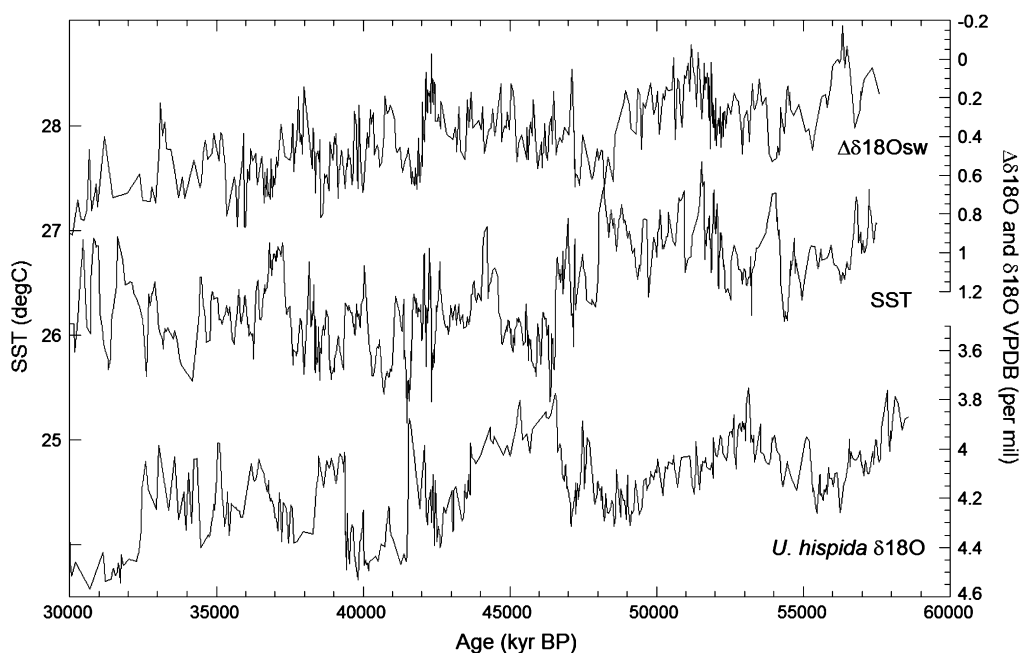


Fig. 4. Phasing between the surface and the deep-water signals. MD98–2181 planktonic SST and $\Delta\delta^{18}\text{O}$ and benthic $\delta^{18}\text{O}_{\text{VPDB}}$.

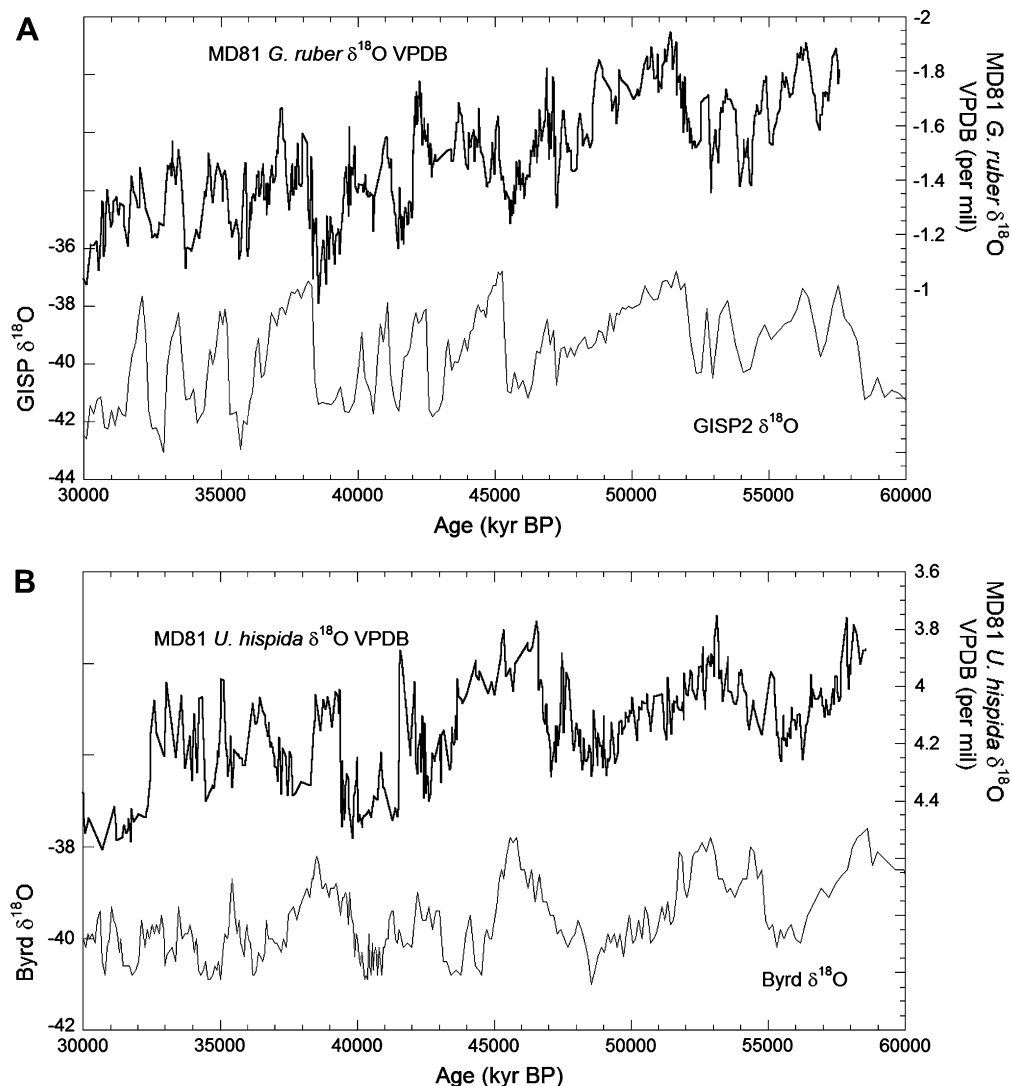


Fig. 5. (A) GISP2 $\delta^{18}\text{O}$ and MD98-2181 $G. ruber \delta^{18}\text{O}_{\text{VPDB}}$ data; (B) Byrd $\delta^{18}\text{O}$ and MD98-2181 $U. hispida \delta^{18}\text{O}$ plotted with respect to the GISP2 age scale of Blunier and Brook (2001).

1996; Boyle, 2000), and potentially responding to internal instabilities and/or external forcing (such as ice dynamics and/or ice-volume fluctuations) initiated in either hemisphere (Stocker et al., 1992; Broecker, 1994; Kanfoush et al., 2000; Seidov and Maslin, 2001; Weaver et al., 2003). Computer simulations suggest that the imbalances between northern- and southern-sourced water masses are the primary agent for millennial climate oscillations (Stocker et al., 1992) driven by changes in AABW (Toggweiler and Samuels, 1995; Knorr and Lohmann, 2003) or NADW (Knutti et al., 2004). Studies by Charles et al. (1996), Ninnemann and Charles (2002), Skinner et al. (2003), Pahnke and Zahn (2005) and Martrat et al. (2007) have interpreted benthic $\delta^{18}\text{O}$ and $\delta^{13}\text{C}$ oscillations from the North Atlantic and South Atlantic and the southwest Pacific to reflect changes in the dominance of AAIW and AABW versus NADW. The western tropical Pacific now also fits this global picture. MD98-2181 $\delta^{18}\text{O}_c$ benthic oscillations recorded in the western Pacific MD98-2181 show warming of the Pacific Deep Water with a potential reduction of salinity coinciding with warming over the Antarctic continent and enhanced AAIW and AABW production. Colder/more saline Pacific Deep Water and Antarctic air temperatures appear to coincide with increased influence of NADW in the Southern Hemisphere. There are still some chronological uncertainties, but a growing number of studies

now link the oceanographic changes seen in the Atlantic and the Pacific to the ice core records of temperature change over Greenland and Antarctica.

5.4. Southern Ocean origin of abrupt climate change?

Ahn and Brook (2007) found that CO_2 concentrations and Antarctic temperatures were positively correlated over millennial-scale climate cycles, implying a strong connection to Southern Ocean processes. Atmospheric CO_2 concentrations are influenced by oceanic dynamical and biological processes in the Southern Ocean (Russell et al., 2006). Fig. 6 shows a comparison of the MD98-2181 benthic $\delta^{18}\text{O}$ with the Antarctic atmospheric temperature and CO_2 history from Byrd Station. The atmospheric and deep-water temperatures appear to begin warming and reach peak values in advance of rising CO_2 . This observation is consistent among the millennial CO_2 fluctuations but is dependent upon the accuracy of the deep sea and Antarctic age models. If these age models are correct it would imply that changing temperatures in the Southern Ocean were involved in producing the observed CO_2 changes.

The MD98-2181 benthic record and the Antarctic record of atmospheric CO_2 may be associated through changes in the Southern Ocean overturning temperatures (through Southern

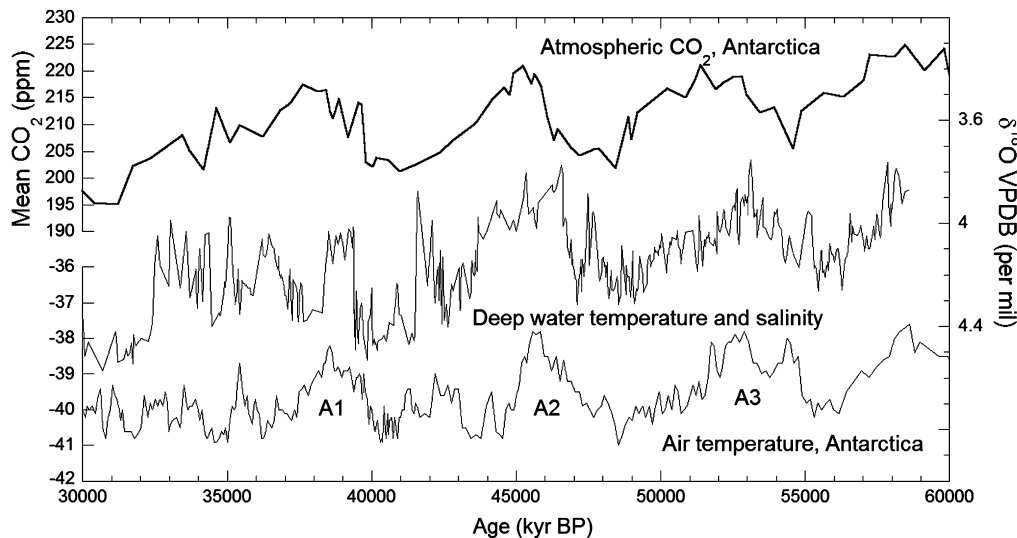


Fig. 6. Byrd $\delta^{18}\text{O}$, Byrd atmospheric CO_2 and MD98-2181 *U. hispidus* $\delta^{18}\text{O}$ plotted with respect to the GISP2 age scale of Blunier and Brook (2001) and Ahn and Brook (2007).

Ocean control of CO_2 potentially by variation in sea ice cover). The Southern Ocean is the meeting point for the Pacific, Atlantic and Indian Oceans. The strong westerly winds drive the Antarctic Circumpolar Current and the resulting divergence drives upwelling. Due to the sloping isopycnals and the tendency for water masses to mix along these isopycnals, water at depths of up to 2–3 km can be ventilated to the surface (Russell et al., 2006). Therefore climate signals originating in the Southern Ocean can be amplified and transmitted globally via the ACC and the atmosphere.

More details of the extent of regional variability within Antarctica are now beginning to appear. Fischer et al. (2007) presented evidence for large changes in the flux of non-sea salt Ca^{++} , a proxy for the strength of winds carrying dust from Patagonian to the EDML site. There is a strong correlation between the EDML air temperatures and the dust source wind strength during Antarctica warm/cold events. The large changes in dust indicate changes in the westerly wind strength just before the air temperatures began to increase. Regional changes in the westerly wind strength and corresponding changes in sea ice extent may have resulted in reduced stratification of the Southern Ocean and greater exchange of CO_2 from the ocean to the atmosphere. Against a background of increasingly glacial climate on the way towards the LGM and of changing orbital and solar forcing, regional changes such as wind strength around Antarctica may be significant to the onset of abrupt climate change events on these millennial timescales.

6. Conclusions

There was close temporal correspondence between the MD98-2181 planktonic $\delta^{18}\text{O}_c$, Mg/Ca SST and $\Delta\delta^{18}\text{O}_{\text{sw}}$ variations and temperature changes over Greenland during MIS 3. Sea surface temperatures and salinity in the western Pacific were changing in response to varying strength of the Asian monsoon. Our MD98-2181 results indicate higher salinities and colder SSTs in the WPWP during the Greenland stadials of MIS 3. This tropical behavior appears to reflect a southerly migration of the mean position of the ITCZ together with a weakened East Asian summer monsoon and decreased summer precipitation. The extent to which these changes were also associated with the frequency of ENSO in the Pacific remains an open question.

In contrast to the planktonic record from MD98-2181, the benthic $\delta^{18}\text{O}_c$ record documents large millennial-scale oscillations

that correlate closely with the Antarctic surface temperature history and reflect shifting deep-water temperatures and perhaps salinity and minor glacial–eustatic changes. Such changes in deepwater properties are interpreted to reflect changes in the source water temperatures (and perhaps salinity) at the site where Upper Circumpolar Deep Water forms in the Antarctic Ocean.

The surface and the deep-water climate signals (adjusted for travel time) in the MD98-2181 are anti-phased during MIS 3. These combined planktonic and benthic records from MD98-2181 thus provide both northern and southern hemispheric climate records and verify the anti-phased relationship associated with a bi-polar seesaw oceanographic behavior throughout MIS 3. There are still some chronological issues to be resolved, but a growing number of studies link oceanographic changes seen in the Atlantic and the Pacific to the swings in air temperature over Greenland and Antarctica and the data from MD98-2181 fits this interpretation. The origin of abrupt climate swings during MIS 3 remains unclear but the fact that the deep Pacific was undergoing contemporaneous changes in temperature with those in Antarctica implicates the Pacific as a major factor in the large scale climate oscillations during the Last Glacial.

References

- Ahn, J.H., Brook, E.J., 2007. Atmospheric CO_2 and climate from 65 to 30 ka BP. *Geophysical Research Letters* 34. doi:10.1029/2007GL029551.
- Altabet, M.A., Higginson, M.J., Murray, D.W., 2002. The effect of millennial-scale changes in Arabian Sea denitrification on atmospheric CO_2 . *Nature* 415, 159–162.
- Anand, P., Elderfield, H., Conte, M.H., 2003. Calibration of Mg/Ca thermometry in planktonic foraminifera from a sediment trap time series. *Paleoceanography* 18. doi:10.1029/2002PA000846.
- Arz, H.W., Lamy, F., Ganopolski, A., Nowaczyk, N., Pätzold, J., 2007. Dominant Northern Hemisphere climate control over millennial-scale glacial sea-level variability. *Quaternary Science Reviews* 26, 312–321.
- Barbante, C., Barnola, J.M., Becagli, S., Beer, J., Bigler, M., Boutron, C., Blunier, T., Castellano, E., Cattani, O., Chappellaz, J., Dahl-Jensen, D., Debet, M., Delmonte, B., Dick, D., Falourd, S., Faria, S., Federer, U., Fischer, H., Freitag, J., Frenzel, A., Fritzsche, D., Fundel, F., Gabrielli, P., Gaspari, V., Gersonde, R., Graf, W., Grigoriev, D., Hamann, I., Hansson, M., Hoffmann, G., Hutterli, M.A., Huybrechts, P., Isaksson, E., Johnsen, S., Jouzel, J., Kaczmarek, M., Karlin, T., Kaufmann, P., Kipfstuhl, S., Kohno, M., Lambert, F., Lambrecht, A., Lambrecht, A., Landais, A., Lawer, G., Leuenberger, M., Littot, G., Loulergue, L., Luthi, D., Maggi, V., Marino, F., Masson-Delmotte, V., Meyer, H., Miller, H., Mulvaney, R., Narcisi, B., Oerlemans, J., Oerter, H., Parrenin, F., Petit, J.R., Raisbeck, G., Raynaud, D., Rothlisberger, R., Ruth, U., Rybak, O., Severi, M., Schmitt, J., Schwander, J., Siegenthaler, U., Siggaard-Anderesen, M.L., Spahni, R., Steffensen, J.P., Stenni, B., Stocker, T.F., Tison, J.L., Traversi, R., Udisti, R., Valero-

- Delgado, F., van den Broeke, M.R., van de Wal, R.S.W., Wagenbach, D., Wegner, A., Weiler, K., Wilhelms, F., Winther, J.G., Wolff, E., 2006. One-to-one coupling of glacial climate variability in Greenland and Antarctica. *Nature* 444, 195–198.
- Behl, R.J., Kennett, J.P., 1996. Brief interstadial events in the Santa Barbara basin, NE Pacific, during the past 60 kyr. *Nature* 379, 243–246.
- Bemis, B.E., Spero, H.J., Bijma, J., Lea, D.W., 1998. Reevaluation of the oxygen isotopic composition of planktonic foraminifera: experimental results and revised paleotemperature equations. *Paleoceanography* 13, 150–160.
- Blunier, T., Brook, E.J., 2001. Timing of millennial-scale climate change in Antarctica and Greenland during the last glacial period. *Science* 291, 109–112.
- Blunier, T., Schwander, J., Stauffer, B., Stocker, T., Dallenbach, A., Indermuhle, A., Tschumi, J., Chappellaz, J., Raynaud, D., Barnola, J.M., 1997. Timing of the Antarctic cold reversal and the atmospheric CO₂ increase with respect to the Younger Dryas event. *Geophysical Research Letters* 24, 2683–2686.
- Blunier, T., Chappellaz, J., Schwander, J., Dallenbach, A., Stauffer, B., Stocker, T.F., Raynaud, D., Jouzel, J., Clausen, H.B., Hammer, C.U., Johnsen, S.J., 1998. Asynchrony of Antarctic and Greenland climate change during the last glacial period. *Nature* 394, 739–743.
- Boersma, A., 1984. *A Handbook of Common Tertiary Uvigerina*. Microclimate Press, Stony Point, NY.
- Boyle, E.A., 2000. Is ocean thermohaline circulation linked to abrupt stadial/interstadial transitions? *Quaternary Science Reviews* 19, 255–272.
- Broecker, W.S., 1994. Massive iceberg discharges as triggers for global climate change. *Nature* 372, 421–424.
- Broecker, W.S., 1998. Paleocirculation during the last deglaciation: a bipolar seesaw? *Paleoceanography* 13, 119–121.
- Broecker, W., Barker, S., Clark, E., Hajdas, I., Bonani, G., Stott, L., 2004. Ventilation of the Glacial Deep Pacific Ocean. *Science* 306, 1169–1172.
- Burns, S.J., Fleitmann, D., Matter, A., Kramers, J., Al-Subary, A.A., 2003. Indian Ocean climate and an absolute chronology over Dansgaard/Oeschger events 9 to 13. *Science* 301, 1365–1367.
- Butzin, M., Prange, M., Lohmann, G., 2005. Radiocarbon simulations for the glacial ocean: the effects of wind stress, Southern Ocean sea ice and Heinrich events. *Earth and Planetary Science Letters* 235, 45–61.
- Chappell, J., 2002. Sea level changes forced ice breakouts in the Last Glacial cycle: new results from coral terraces. *Quaternary Science Reviews* 21, 1229–1240.
- Charles, C.D., Lynch-Stieglitz, J., Ninnemann, U.S., Fairbanks, R.G., 1996. Climate connections between the hemispheres revealed by deep sea sediment core/ice core correlations. *Earth and Planetary Science Letters* 142, 19–27.
- Clement, A.C., Seager, R., Cane, M.A., 2000. Suppression of El Niño during the Mid-Holocene by changes in the Earth's orbit. *Paleoceanography* 15.
- Cruz, F.W., Burns, S.J., Karmann, I., Sharp, W.D., Vuille, M., Cardoso, A.O., Ferrari, J.A., Dias, P.L.S., Viana, O., 2005. Insolation-driven changes in atmospheric circulation over the past 116,000 years in subtropical Brazil. *Nature* 434, 63–66.
- Dannenmann, S., Linsley, B.K., Oppo, D.W., Rosenthal, Y., Beaufort, L., 2003. East Asian monsoon forcing of suborbital variability in the Sulu Sea during Marine Isotope Stage 3: link to Northern Hemisphere climate. *Geochemistry Geophysics Geosystems* 4. doi:10.1029/2002GC000390.
- Duplessy, J.C., Arnold, M., Shackleton, N.J., Kallel, N., Labeyrie, L., Juillet-Leclerc, A., 1988. Changes in the rate of ventilation of intermediate and deep-water masses in the Pacific-Ocean during the last deglaciation. *Chemical Geology* 70, 108.
- Fairbanks, R.G., Evans, M.N., Rubenstone, J.L., Mortlock, R.A., Broad, K., Moore, M.D., Charles, C.D., 1997. Evaluating climate indices and their geochemical proxies measured in corals. *Coral Reefs* 16, S93–S100.
- Fischer, H., Fundel, F., Ruth, U., Twarloh, B., Wegner, A., Udister, R., Becagli, S., Castellano, E., Morganti, A., Severi, M., Wolff, E., Littot, G., Rothlisberger, R., Mulvaney, R., Hutterli, M.A., Kaufmann, P., Federer, U., Lambert, F., Bigler, M., Hansson, M., Jonsell, U., de Angelis, M., Bouton, C., Siggaard-Andersen, M.L., Steffensen, J.P., Barbante, C., Gaspari, V., Gabrielli, P., Wagenbach, D., 2007. Reconstruction of millennial changes in dust emission, transport and regional sea ice coverage using the deep EPICA ice cores from the Atlantic and Indian Ocean sector of Antarctica. *Earth and Planetary Science Letters* 260, 340–354.
- Genty, D., Blamart, D., Ouahdi, R., Gilmour, M., Baker, A., Jouzel, J., Van-Exter, S., 2003. Precise dating of Dansgaard-Oeschger climate oscillations in western Europe from stalagmite data. *Nature* 421, 833–837.
- Gordon, A.L., 2005. Oceanography of the Indonesian Seas and their throughflow. *Oceanography* 18, 14–27.
- Haug, G.H., Hughen, K.A., Sigman, D.M., Peterson, L.C., Rohl, U., 2001. Southward migration of the Intertropical Convergence Zone through the Holocene. *Science* 293, 1304–1308.
- Hemming, S.R., 2004. Heinrich events: massive Late Pleistocene detritus layers of the North Atlantic and their global climate imprint. *Reviews of Geophysics* 42, 43.
- Jin, F.-F., Neelin, J.D., Ghil, M., 1994. El Niño on the Devil's staircase: annual subharmonic steps to chaos. *Science* 264, 70–72.
- Jouzel, J., Vaikmae, R., Petit, J.R., Martin, M., Duclos, Y., Stievenard, M., Lorius, C., Toots, M., Melieres, M.A., Burckle, L.H., Barkov, N.I., Kotlyakov, V.M., 1995. The 2-step shape and timing of the last deglaciation in Antarctica. *Climate Dynamics* 11, 151–161.
- Kanfoush, S.L., Hodell, D.A., Charles, C.D., Guilderson, T.P., Mortyn, P.G., Ninnemann, U.S., 2000. Millennial-scale instability of the Antarctic ice sheet during the last glaciation. *Science* 288, 1815–1818.
- Kawahata, H., 2005. Stable isotopic composition of two morphotypes of Globigerinoides ruber (white) in the subtropical gyre in the North Pacific. *Paleontological Research* 9, 27–35.
- Kawahata, H., Nishimura, A., Gagan, M.K., 2002. Seasonal change in foraminiferal production in the western equatorial Pacific warm pool: evidence from sediment trap experiments. *Deep Sea Research Part II: Topical Studies in Oceanography* 49, 2783–2800.
- Kawamura, K., Parrenin, F., Lisiecki, L., Uemura, R., Vimeux, F., Severinghaus, J.P., Hutterli, M.A., Nakazawa, T., Aoki, S., Jouzel, J., Raymo, M.E., Matsumoto, K., Nakata, H., Motoyama, H., Fujita, S., Goto-Azuma, K., Fujii, Y., Watanabe, O., 2007. Northern Hemisphere forcing of climatic cycles in Antarctica over the past 360,000 years. *Nature* 448, 912–916.
- Key, R.M., Kozyr, A., Sabine, C.L., Lee, K., Wanninkhof, R., Bullister, J.L., Feely, R.A., Millero, F.J., Mordy, C., Peng, T.H., 2004. A global ocean carbon climatology: results from Global Data Analysis Project (GLODAP). *Global Biogeochemical Cycles* 18. doi:10.1029/2004GB002247.
- Knorr, G., Lohmann, G., 2003. Southern Ocean origin for the resumption of Atlantic thermohaline circulation during deglaciation. *Nature* 424, 532–536.
- Knutti, R., Flückiger, J., Stocker, T.F., Timmermann, A., 2004. Strong hemispheric coupling of glacial climate through freshwater discharge and ocean circulation. *Nature* 430, 851–856.
- Koutavas, A., Lynch-Stieglitz, J., Marchitto, T.M., Sachs, J.P., 2002. El Niño-like pattern in ice age tropical Pacific sea surface temperature. *Science* 297, 226–230.
- Koutavas, A., deMenocal, P.B., Olive, G.C., Lynch-Stieglitz, J., 2006. Mid-Holocene El Niño–Southern Oscillation (ENSO) attenuation revealed by individual foraminifera in eastern tropical Pacific sediments. *Geology* 34, 993–996.
- Labracherie, M., Labeyrie, L.D., Duprat, J., Bard, E., Arnold, M., Pichon, J.J., Duplessy, J.C., 1989. The last deglaciation in the Southern Ocean. *Paleoceanography* 4, 629–638.
- Lea, D.W., Pak, D.K., Spero, H.J., 2000. Climate impact of late quaternary equatorial Pacific sea surface temperature variations. *Science* 289, 1719–1724.
- Leduc, G., Vidal, L., Tachikawa, K., Rostek, F., Sonzogni, C., Beaufort, L., Bard, E., 2007. Moisture transport across Central America as a positive feedback on abrupt climatic changes. *Nature* 445, 908–911.
- Leduc, G., Vidal, L., Tachikawa, K., Bard, E., 2009. ITCZ rather than ENSO signature for abrupt climate changes across the tropical Pacific? *Quaternary Research* 72, 123–131.
- Martrat, B., Grimalt, J.O., Lopez-Martinez, C., Cacho, I., Sierro, F.J., Flores, J.A., Zahn, R., Canals, M., Curtis, J.H., Hodell, D.A., 2004. Abrupt temperature changes in the Western Mediterranean over the past 250,000 years. *Science* 306, 1762–1765.
- Martrat, B., Grimalt, J.O., Shackleton, N.J., de Abreu, L., Hutterli, M.A., Stocker, T.F., 2007. Four climate cycles of recurring deep and surface water destabilizations on the Iberian margin. *Science* 317, 502–507.
- McCave, I.N., Carter, L., Hall, I.R., 2008. Glacial–interglacial changes in water mass structure and flow in the SW Pacific Ocean. *Quaternary Science Reviews* 27, 1886–1908.
- Meehl, G.A., Washington, W.M., 1996. El Niño-like climate change in a model with increased atmospheric CO₂ concentrations. *Nature* 382, 56–60.
- Mix, A.C., Lund, D.C., Pisias, N.G., Boden, P., Bornmalm, L., Lyle, M., Pike, J., 1999. Rapid climate oscillations in the northeast Pacific during the last deglaciation reflect northern and Southern Hemisphere sources. *Geophysical Monograph*.
- Morimoto, M., Abe, O., Kayanne, H., Kurita, N., Matsumoto, E., Yoshida, N., 2002. Salinity records for the 1997–98 El Niño from Western Pacific corals. *Geophysical Research Letters* 29. doi:10.1029/2001GL013521.
- Muller, J., Kylander, M., Wust, R.A.J., Weiss, D., Martinez-Cortizas, A., LeGrande, A.N., Jennerjahn, T., Behling, H., Anderson, W.T., Jacobson, G., 2008. Possible evidence for wet Heinrich phases in tropical NE Australia: the Lynch's Crater deposit. *Quaternary Science Reviews* 27, 468–475.
- Newton, A., Thunell, R., Stott, L., 2006. Climate and hydrographic variability in the Indo-Pacific Warm Pool during the last millennium. *Geophysical Research Letters* 33, 5.
- Ninnemann, U.S., Charles, C.D., 2002. Changes in the mode of Southern Ocean circulation over the last glacial cycle revealed by foraminiferal stable isotopic variability. *Earth and Planetary Science Letters* 201, 383–396.
- Nittrouer, C.A., Brunskill, G.J., Figueiredo, A.G., 1995. Importance of tropical coastal environments. *Geo-Marine Letters* 15, 121–126.
- Oppo, D.W., Schmidt, G.A., LeGrande, A.N., 2007. Seawater isotope constraints on tropical hydrology during the Holocene. *Geophysical Research Letters* 34.
- Ostlund, W.G., Stuiver, M., 1980. GEOSECS Pacific radiocarbon. *Radiocarbon* 22, 25–53.
- Pahnke, K., Zahn, R., 2005. Southern hemisphere water mass conversion linked with North Atlantic climate variability. *Science* 307, 1741–1746.
- Pelejero, C., Grimalt, J.O., Heilig, S., Kienast, M., Wang, L.J., 1999. High-resolution U-37(K) temperature reconstructions in the South China Sea over the past 220 kyr. *Paleoceanography* 14, 224–231.
- Raisbeck, G.M., Yiou, F., Jouzel, J., Stocker, T.F., 2007. Direct north–south synchronization of abrupt climate change record in ice cores using beryllium 10. *Climate of the Past* 3, 541–547.
- Rintoul, S.R., Sokolov, S., Church, J.A., 2001. *Ocean Circulation and Climate: Observing and Modelling the Global Ocean*. Academic Press, London.
- Rohling, E.J., Marsh, R., Wells, N.C., Siddall, M., Edwards, N.R., 2004. Similar meltwater contributions to glacial sea level changes from Antarctic and northern ice sheets. *Nature* 430, 1016–1021.
- Russell, J.L., Dixon, K.W., Gnanadesikan, A., Stouffer, R.J., Toggweiler, J.R., 2006. The Southern Hemisphere westerlies in a warming world: propping open the door to the deep ocean. *Journal of Climate* 19, 6382–6390.
- Schulz, H., von Rad, U., Erlenkeuser, H., 1998. Correlation between Arabian Sea and Greenland climate oscillations of the past 110,000 years. *Nature* 393, 54–57.
- Seidov, D., Maslin, M., 2001. Atlantic Ocean heat piracy and the bipolar climate seesaw during Heinrich and Dansgaard-Oeschger events. *Journal of Quaternary Science* 16, 321–328.

- Shackleton, N.J., Hall, M.A., Vincent, E., 2000. Phase relationships between millennial-scale events 64,000–24,000 years ago. *Paleoceanography* 15, 565–569.
- Siddall, M., Rohling, E.J., Almogi, L.A., Hemleben, C., Meischner, D., Schmelzer, I., Smeed, D.A., 2003. Sea-level fluctuations during the last glacial cycle. *Nature* 423, 853–858.
- Sikes, E.L., Samson, C.R., Guilderson, T.P., Howard, W.R., 2000. Old radiocarbon ages in the southwest Pacific Ocean during the last glacial period and deglaciation. *Nature* 405, 555–559.
- Sirocko, F., Leuschner, D., Staubwasser, M., Maley, J., Heusser, L., 1999. High-frequency oscillations of the last 70,000 years in the tropical/subtropical and polar climates, in: *Mechanisms of Global Climate Change at Millennial Time Scales*. Geophysical Monograph Series. American Geophysical Union, Washington, pp. 113–126.
- Skinner, L.C., Elderfield, H., 2007. Rapid fluctuations in the deep North Atlantic heat budget during the last glacial period. *Paleoceanography* 22. doi:10.1029/2006PA001338.
- Skinner, L.C., Shackleton, N.J., 2005. An Atlantic lead over Pacific deep-water change across Termination I: implications for the application of the marine isotope stage stratigraphy. *Quaternary Science Reviews* 24, 571–580.
- Skinner, L.C., Shackleton, N.J., Elderfield, H., 2003. Millennial-scale variability of deep-water temperature and delta O-18(dw) indicating deep-water source variations in the Northeast Atlantic, 0–34 cal. ka BP. *Geochemistry Geophysics Geosystems* 4. doi:10.1029/2003GC000585.
- Sowers, T., Bender, M., 1995. Climate records covering the last deglaciation. *Science* 269, 210–214.
- Stocker, T.F., 1998. Climate change – The seesaw effect. *Science* 282, 61–62.
- Stocker, T.F., Johnsen, S.J., 2003. A minimum thermodynamic model for the bipolar seesaw. *Paleoceanography* 18. doi:10.1029/2003PA000920.
- Stocker, T.F., Wright, D.G., Mysak, L.A., 1992. A zonally averaged, coupled ocean atmosphere model for paleoclimate studies. *Journal of Climate* 5, 773–797.
- Stott, L., Poulsen, C., Lund, S., Thunell, R., 2002. Super ENSO and global climate oscillations at millennial time scales. *Science* 297, 222–226.
- Stott, L., Cannariato, K., Thunell, R., Haug, G.H., Koutavas, A., Lund, S., 2004. Decline of surface temperature and salinity in the western tropical Pacific Ocean in the Holocene epoch. *Nature* 431, 56–59.
- Stott, L., Timmermann, A., Thunell, R., 2007. Southern Hemisphere and deep-sea warming led deglacial atmospheric CO₂ rise and tropical warming. *Science* 318, 435–438.
- Timmermann, A., Jin, F.F., Collins, M., 2004. Intensification of the annual cycle in the tropical Pacific due to greenhouse warming. *Geophysical Research Letters* 31.
- Timmermann, A., Timm, O., Stott, L., Menviel, L., 2009. The roles of CO₂ and orbital forcing in driving southern hemispheric temperature variations during the last 21 000 yrs. *Journal of Climate* 22, 1626–1640.
- Toggweiler, J.R., Samuels, B., 1995. Effect of sea-ice on the salinity of Antarctic bottom waters. *Journal of Physical Oceanography* 25, 1980–1997.
- Tziperman, E., Stone, L., Cane, M.A., Jarosh, H., 1994. El Niño chaos: overlapping of resonances between the seasonal cycle and the Pacific Ocean–atmosphere oscillator. *Science* 264, 72–74.
- van de Flierdt, T., Frank, M., Halliday, A.N., Hein, J.R., Hattendorf, B., Gunther, D., Kubik, P.W., 2004. Deep and bottom water export from the Southern Ocean to the Pacific over the past 38 million years. *Paleoceanography* 19. doi:10.1029/2003PA000923.
- Wang, Y.J., Cheng, H., Edwards, R.L., An, Z.S., Wu, J.Y., Shen, C.C., Dorale, J.A., 2001. A high-resolution absolute-dated Late Pleistocene monsoon record from Hulu Cave, China. *Science* 294, 2345–2348.
- Wang, X.F., Auler, A.S., Edwards, R.L., Cheng, H., Cristalli, P.S., Smart, P.L., Richards, D.A., Shen, C.C., 2004. Wet periods in northeastern Brazil over the past 210 kyr linked to distant climate anomalies. *Nature* 432, 740–743.
- Weaver, A.J., Saenko, O.A., Clark, P.U., Mitrovica, J.X., 2003. Meltwater pulse 1A from Antarctica as a trigger of the Bolling–Allerod warm interval. *Science* 299, 1709–1713.
- Xie, S.-P., Okumura, Y., Miyama, T., Timmermann, A., 2008. Influences of Atlantic climate change on the tropical Pacific via the Central American Isthmus. *Journal of Climate* 21, 3914–3928.